

Nuclear Spin-Lattice Relaxation in CaF₂ Crystals via Paramagnetic Centers*†

D. TSE‡ AND I. J. LOWE

Department of Physics, University of Pittsburgh, Pittsburgh, Pennsylvania

(Received 13 September 1967)

The results of nuclear spin-lattice relaxation-time measurements in the laboratory reference frame (T_1) and the rotating reference frame (T_1^r), made on F¹⁹ nuclei in CaF₂ crystals doped either with Eu³⁺, Ce³⁺, or Mn²⁺ paramagnetic centers, are reported. From 0.25 to 0.36 of the Debye temperature, values of the correlation time τ_c are found from T_1^r minima for Mn²⁺ ions. Over this range $\tau_c \propto T^{-3.2 \pm 0.1}$, compared to $T^{-3.2}$ computed from Leushin's theory. For Eu³⁺ over 0.15 to 0.19 of the Debye temperature, measurements yield $\tau_c \propto T^{-4.9 \pm 0.1}$, compared to $T^{-4.7}$ computed from Leushin's theory. From the T_1 data for a Mn²⁺-doped CaF₂ crystal, a value of 1.9×10^{-12} cm²/sec for the spin-diffusion constant D is computed. From the T_1 data for a Eu³⁺-doped CaF₂ crystal, D is computed to be 1.2×10^{-12} cm²/sec. A NMR measurement of the effective number of paramagnetic centers per unit volume, N_p , increases the measured D to 2.6×10^{-12} cm²/sec. The computed value of D (Lowe and Gade) is 5.1×10^{-12} cm²/sec. Indirect evidence leads to the conclusion that the spin-diffusion barrier radius is at least a factor of 2 smaller than predicted by Rorschach's formula. In the short- τ_c region, T_1 and T_1^r , are found to be field-independent, with $T_1^r/T_1 > 1$. The experimental data are consistent with $T_1 \propto B_0^{1/2} \tau_c^{1/4} N_p^{-1}$ (diffusion-limited region), $T_1 \propto B_0 \tau_c^{1/2} N_p^{-4/3}$ (diffusion-vanishing region). The initial decay of the magnetization in the measurements of T_1^r is found to be proportional to $t^{1/2}$ in the long-correlation-time region. The coefficient of $t^{1/2}$ is used to obtain an experimental value for N_p that is $\frac{1}{2}$ as large as the value supplied by the manufacturer of the crystal.

I. INTRODUCTION

MANY experiments have been done to test the validity of the theory of nuclear spin-lattice relaxation via paramagnetic centers.¹⁻⁵ In the first experimental work, the proton system in hydrated alums was used. Since the water molecules are known to have other effective relaxation mechanisms,^{6,7} the effect of the paramagnetic centers would tend to be obscured. In 1958 Winter⁸ found, that for the diffusion-limited case, the inverse of the nuclear spin-lattice relaxation time T_1 was proportional to the square root of the applied magnetic field, if the correlation time τ_c of the paramagnetic center was field-independent. However, other authors⁹ have found it necessary to make τ_c field-dependent in order to obtain agreement between theory and experiment. The most recent examination of the field dependence of T_1 was made by Goldman.⁹ His data indicated that the field-dependence of T_1 was not the same in high field as in low field. We

have shown, in the preceding paper (hereafter referred to as LT), that when the spin system relaxes in a relatively low magnetic field, the relaxation time T_1 may have a new magnetic field dependence, different from either the diffusion-limited case or the rapid-diffusion case.

Usually, the magnitudes of τ_c of the various types of paramagnetic centers in a host lattice vary widely from species to species, even at a given temperature. When the paramagnetic species is known, information about τ_c for a T_1 calculation can sometimes be found from electron spin-resonance data, assuming that the spin-lattice relaxation time of the paramagnetic centers is the same as τ_c . When crystals are not artificially doped, the contributions from numerous intrinsic species can make the determination of τ_c hopelessly complicated.¹⁰ This difficulty can be sidestepped by using samples that are artificially doped with known paramagnetic centers, the doping level being high enough to dominate the effects of background paramagnetic centers.

In this paper we present measurements of nuclear spin-lattice relaxation times of crystals doped with paramagnetic centers. We have tried to avoid some of the sources of error and difficulty in interpretation listed above, and we have looked for the diffusion-vanishing case predicted in LT. To eliminate the uncertainty in τ_c , we carried out our measurements on crystals artificially doped with paramagnetic centers. To avoid any possible magnetic field dependence of τ_c upon nuclear spin-lattice relaxation times, measurements of T_1^r , the nuclear spin-lattice relaxation time in the rotating reference frame, were made.

* This paper is based upon work presented by D. Tse to the Department of Physics, University of Pittsburgh, in partial fulfillment of the requirements for a Ph.D. degree.

† This work was supported by the U.S. Air Force Office of Scientific Research, Grant No. 196-63.

‡ Present address: Department of Physics, Columbia University, New York, N.Y.

¹ N. Bloembergen, *Physica* **15**, 386 (1949).

² T. Beal and J. Hutton, *Phys. Letters* **15**, 210 (1965).

³ S. M. Day, E. Otsuka, and B. Josephson, Jr., *Phys. Rev.* **137**, 108 (1965).

⁴ S. M. Day, G. B. Grimes Jr., and W. Weatherford, *Phys. Rev.* **139**, 515 (1965).

⁵ B. Josephson and M. W. P. Strangberg, *J. Phys. Chem. Solids* **23**, 67 (1962).

⁶ A. H. Cooke and L. F. Drain, *Proc. Phys. Soc. (London)* **65**, 894 (1952).

⁷ D. Look, M. S. thesis, University of Minnesota, Minneapolis, 1962 (unpublished).

⁸ J. Winter, *Compt. Rend.* **249**, 2192 (1959).

⁹ M. Goldman, *Phys. Rev.* **138**, 1675 (1965).

¹⁰ (a) T. Kushida and A. H. Silver, *Phys. Rev.* **137**, 1591 (1965); (b) D. R. Huffman and M. H. Norwood, *ibid.* **117**, 709 (1960).

II. EXPERIMENTAL PROCEDURE

A. Samples

Calcium fluoride (CaF_2) was chosen as the host material for the relaxation experiments for the reasons enumerated below.

(a) CaF_2 has a high Debye temperature^{10a} (510°K), and for experiments carried out at room temperature and below, the nuclei may be assumed fixed in a rigid lattice for computational purposes. Further, the contribution to T_1 due to the modulation of the nuclear coordinates by the lattice vibrations is many orders of magnitude smaller than the contributions to T_1 due to paramagnetic centers in the crystal.¹

(b) The only stable isotope of fluorine (F^{19}) has an angular momentum of $\hbar/2$ and thus no quadrupole moment. The existence of one isotope makes the calculation of the spin-diffusion constant somewhat easier than the case where there are several isotopes. The lack of a quadrupole moment means that one need not worry about the effects of spin-lattice relaxation or line broadening due to the quadrupole moment.

(c) Ca^{48} is the only isotope of calcium that has a spin different from zero, and it is 0.14% abundant and has a very small magnetic moment. Therefore, it need not be considered in computing spin-diffusion constants.

(d) The fluorine nuclei form a simple cubic structure which simplifies the evaluation of the spin-diffusion constant D .

(e) Stable fluorides of the iron group and rare-earth group are available for doping the CaF_2 crystals.

Measurements were made on 15 different CaF_2 crystals. The one containing Eu^{3+} paramagnetic centers was obtained commercially.¹¹ We grew the eight that were doped with MnF_2 and the six that were doped with CeF_3 . Details of the procedure for growing these crystals can be found in Ref. 12. The crystals were grown from raw natural CaF_2 powder¹³ mixed with a known amount of doping material. MnF_2 has a high vapor pressure at the melting temperature of CaF_2 , so there was some loss of this doping material even though the CaF_2 samples were cooled quickly once they had melted. Because of this quick cooling of the crystals doped with MnF_2 , they were polycrystalline. Room-temperature measurements of the spin-lattice relaxation rate in the laboratory frame yielded T_1^{-1} values that were linearly proportional to the initial charge of doping material. This indicated that with our techniques we were able to produce a set of relaxation centers in the crystal that were a fixed fraction of the initial doping charge. The absolute number of Mn^{2+} centers in our CaF_2 crystal was found by measuring T_1 at room temperature for a commercial¹¹ crystal that had a known Mn^{2+} concentration. This crystal had a T_1

TABLE I. List of CaF_2 crystals for which T_1 and T_1^{-1} measurements are reported.

Sample number	Impurity concentration N_p in $10^{19}/\text{cm}^3$	Average impurity separation R in Å	Crystalline state
Ce^{3+} No. 1	9.8	13.5	Single
Ce^{3+} No. 2	7.4	14.8	Single
Ce^{3+} No. 3	4.8	17.0	Poly.
Ce^{3+} No. 4	3.85	18.4	Poly.
Ce^{3+} No. 5	2.45	21.4	Single
Ce^{3+} No. 6	1.18	27.2	Single
Eu^{3+} No. 1	2.85	20.3	Single
Mn^{2+} No. 1	1.03	28.4	Poly.
Mn^{2+} No. 2	0.83	30.6	Poly.
Mn^{2+} No. 3	0.57	34.8	Poly.
Mn^{2+} No. 4	0.45	37.6	Poly.
Mn^{2+} No. 5	0.31	42.5	Poly.
Mn^{2+} No. 6	0.165	49.5	Poly.
Mn^{2+} No. 7	0.160	50.0	Poly.
Mn^{2+} No. 8	0.056	75.2	Poly.

value that was comparable to our most heavily doped crystal. By carrying out this comparison at room temperature, the linear dependence of T_1^{-1} on N_p was certain. No calibration procedure was thought necessary for the CeF_3 -doped samples, since CeF_3 has a melting point and vapor pressure comparable to that for CaF_2 .

At 10 Mc/sec and room temperature, all doped samples used in our experiments had T_1 's ranging from 10 msec to 0.7 sec. To check on the effect of the paramagnetic centers contained in our starting material, and possibly introduced by our growing procedure, an undoped CaF_2 crystal was grown. It had a T_1 of about 70 sec at room temperature. This indicates that even though unknown impurities in the base materials are inevitable, their effects can be ignored in comparison to those of the added paramagnetic centers. Table I is a list of the 15 crystals and their descriptions. The values of the average impurity separation R are based on the following data: lattice constant of fluorine system: $a=2.73$ Å, formula weight of $\text{CeF}_3=197.12$, formula weight of $\text{EuF}_3=209$, formula weight of $\text{MnF}_2=93$, $R=(3/4\pi N_p)^{1/3}$. The weights of the doping material were ignored in calculating N_p .

B. Methods of Measurement

All measurements reported here were made with a phase-coherent, pulsed, nuclear magnetic resonance spectrometer that was operated at a 10 Mc/sec frequency. Details of this apparatus can be found in Refs. 12 and 14. Nuclear spin-lattice relaxation times were measured in both the laboratory reference frame and the rotating reference frame. The procedures used to get into the rotating reference frame and carry out the measurements are described in Ref. 14. In the

¹¹ Harshaw Chemical Company, Cleveland, Ohio.

¹² D. Tse, Ph. D. thesis, University of Pittsburgh, 1965 (unpublished).

¹³ Fisher Scientific Co., Pittsburgh, Pa.

¹⁴ D. C. Look and I. J. Lowe, J. Chem. Phys. **44**, 2995 (1966).

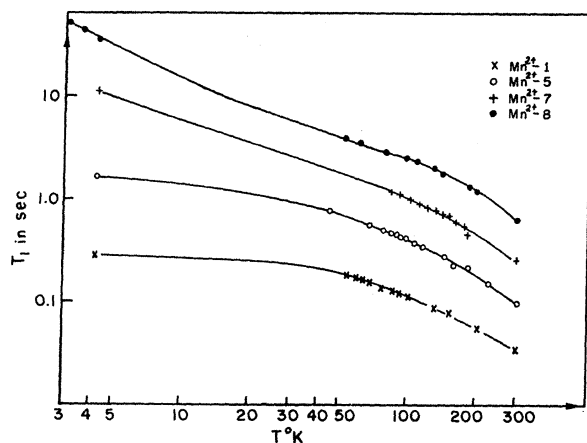


FIG. 1. $\log T_1$ versus $\log T$ for four polycrystalline samples of CaF_2 containing Mn^{2+} centers. Specifications of samples are listed in Table I.

laboratory frame (static field) experiments, the growth of the magnetization along the static magnetic field was measured and obeyed the equation

$$M_z(t) = M_0[1 - \exp(-t/T_1)], \quad (1)$$

where T_1 is the nuclear spin-lattice relaxation time in the laboratory frame and M_0 is the equilibrium magnetization. In the rotating frame (low field) experiment, the decay of the magnetization along the locking magnetic field B_1 was measured and obeyed the equation (except where noted)

$$M^r(t) = M^r(0) \exp(-t/T_1^r), \quad (2)$$

where T_1^r is the nuclear spin-lattice relaxation time in the rotating frame.

The measurements covered the temperature ranges of 2 to 4.2°K and 50 to 300°K. The locking field for the T_1^r measurements ranged from 5 to 25 G.

III. EXPERIMENTAL RESULTS AND THEIR INTERPRETATION

A. Temperature Dependence of the Spin-Lattice Relaxation Time

The temperature dependences of T_1 in high static magnetic field for four Mn^{2+} -doped samples are shown in Fig. 1. The most heavily doped crystal has almost 20 times as many paramagnetic centers as the least heavily doped crystal, and the measured relaxation times span three decades in magnitude. The general behavior of these curves is very similar from 300 to 150°K. At lower temperatures, however, the curves corresponding to the crystals with higher concentrations of paramagnetic centers tend to show a weaker dependence on temperature. This behavior can probably be ascribed to spin-spin interaction among the paramagnetic centers, for the following reason. In the theory of nuclear spin-lattice relaxation due to paramagnetic

centers that was presented in LT, the nuclear T_1 was found to be proportional to some power of $\tau_c/(1+\omega_0^2\tau_c^2)$ for three limiting cases. In this derivation, it was assumed that the motion of the paramagnetic-center spin component that lay along the applied magnetic field B_0 could be described by a correlation time, denoted by τ_c ($\omega_0 = \gamma_n B_0$, where γ_n is the magnetogyric ratio of the nuclei examined). The T_1 's increase with decreasing temperature in Fig. 1. This behavior implies that $\omega_0\tau_c \gg 1$. Thus T_1 is proportional to some power of τ_c . Assuming that the dominant nuclear relaxation mechanism is that of the paramagnetic center, the only temperature dependence of T_1 occurs in the temperature dependence of τ_c . For a given paramagnetic system, τ_c is determined by at least the following two factors: The first is the interaction of the angular momentum of the individual center with the lattice, and this is temperature-dependent. The second is the magnetic interaction among the paramagnetic centers, which to a good approximation is temperature-independent. At high temperatures and low concentrations of paramagnetic centers, the first mechanism is dominant and τ_c , and thus T_1 has the temperature dependence of the first mechanism. This also holds true for dilute systems at low temperatures or heavily doped samples at high enough temperatures. However, for a heavily doped sample at low temperatures, the second mechanism dominates in determining τ_c , and consequently for these samples, T_1 has a weak temperature dependence.

A more fruitful study of the temperature dependence of the nuclear spin-lattice relaxation rate comes from the T_1^r minima obtained in the rotating reference frame experiments. According to Eqs. (72)–(74) of LT, T_1^r is inversely proportional to a power of $\tau_c/(1+\omega_1^2\tau_c^2)$, where $\omega_1/2\pi$ is the nuclear Larmor frequency with respect to the B_1 field in the rotating frame. Thus, for a given value of ω_1 , a T_1^r minimum is obtained when the condition $\omega_1\tau_c \approx 1$ is satisfied. In Fig. 2, measured T_1^r values are plotted as a function of temperature for the Mn^{2+} -doped CaF_2 sample No. 5. The three curves are for measurements made at rotating magnetic field values of 24, 15.6, and 7.6 G. From these T_1^r minima,

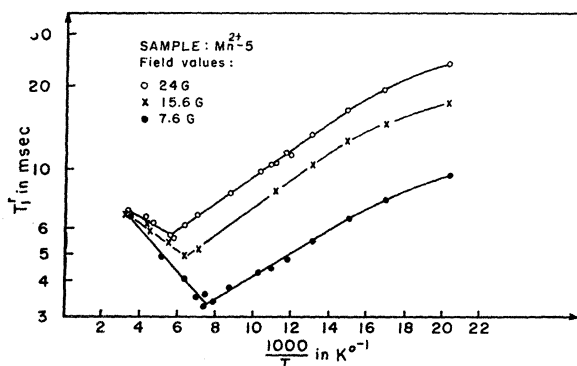


FIG. 2. $\log T_1^r$ versus T^{-1} for Mn^{2+} -doped CaF_2 sample No. 5 for three different values of rotating magnetic field.

the following values of τ_c are calculated:

$$T = 182^\circ\text{K}, \quad \tau_c = 1.65 \times 10^{-6} \text{sec.}$$

$$T = 154^\circ\text{K}, \quad \tau_c = 2.58 \times 10^{-6} \text{sec.}$$

$$T = 128^\circ\text{K}, \quad \tau_c = 5.21 \times 10^{-6} \text{sec.}$$

These τ_c values are plotted against temperature in Fig. 3. The three points lie on a straight line with a slope of -3.2 , which shows that in the range 182 – 128°K , τ_c is inversely proportional to the 3.2 power of T . Mn^{2+} is an S -state ion. Leushin¹⁵ has shown that for an S -state ion imbedded in a diamagnetic crystal with a Debye temperature Θ , the spin-lattice relaxation process is dominated by the two-phonon Raman process, except for $T \ll \Theta$. For such a process, $\tau_c \propto T^7$ for $T \ll \Theta$, and $\tau_c \propto T^2$ for $T > \Theta$. The Debye temperature of CaF_2 is 510°K so that the temperature range of the data covered in Fig. 3 is 0.25 to 0.36Θ . This temperature region lies midway between the above two limiting regions, and our result should also lie somewhere between the two limiting slopes. We have taken Eq. (20) of Leushin's paper¹⁵ for relaxational transition probability and plotted the logarithm of this quantity versus $\log T$. In the temperature range of 0.25 to 0.36Θ , the curve is a straight line with a slope of -3.2 . From this it would seem reasonable to conclude that τ_c for Mn^{2+} in CaF_2 in the temperature range of 128 to 182°K (and higher) is produced by a two-phonon Raman process, and is not measurably influenced by spin-spin interactions. We have carried out an identical analysis for the τ_c versus T data for Eu^{3+} in CaF_2 . These data

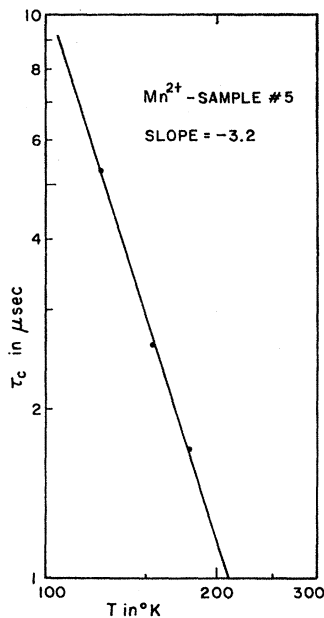


FIG. 3. $\text{Log} \tau_c$ versus $\text{log} T$ for Mn^{2+} -doped CaF_2 sample No. 5.

¹⁵ A. M. Leushin, *Fiz. Tverd. Tela* **5**, 851 (1963) [English transl.: *Soviet Phys.—Solid State* **5**, 623 (1963)].

TABLE II. Calculations of the spin-diffusion constant D from data for τ_c and T_1 for Mn^{2+} -doped CaF_2 sample No. 5.

$T^\circ\text{K}$	τ_c in 10^{-6} sec	T_1 (measured) in sec	D (calculated) in 10^{-12} cm^2/sec
182	1.65 ± 0.05	0.21 ± 0.01	1.9
154	2.58 ± 0.05	0.26 ± 0.01	1.85
128	5.21 ± 0.05	0.31 ± 0.01	1.85

are listed in Table III and cover the temperatures between 0.15 to 0.19Θ . A plot of $\log \tau_c$ versus $\log T$ for these data is a straight line with a slope of -4.9 ± 0.1 . Leushin's theory over this same range yields a straight line with a slope of -4.7 .

The values of τ_c , obtained from the rotating reference frame experiments can be used to determine the dependence of T_1 upon τ_c . A comparison of the τ_c values and the measured T_1 's at the corresponding temperatures for Mn^{2+} shows that within the temperature range 182 – 128°K , T_1 is approximately proportional to $\tau_c^{1/4}$. According to Table I of LT, this $\tau_c^{1/4}$ dependence is characteristic of the diffusion-limited case. For the diffusion-limited case for $\beta/R \ll 1$, it has been derived that (LT and Ref. 14)

$$1/T_1 = \frac{8}{3} \pi N_p (\bar{C})^{1/4} (D)^{3/4}, \quad (3)$$

where

$$\bar{C} = (2/5) S(S+1) \gamma_p^2 \gamma_n^2 \hbar^2 [\tau_c / (1 + \omega_0^2 \tau_c^2)] \quad (4)$$

and

$$\beta = (\bar{C}/D)^{1/4}. \quad (5)$$

γ_p and γ_n are the magnetogyric ratios of the paramagnetic center and nuclei, respectively, S is the spin of the paramagnetic center, and D is an average spin-diffusion constant. All of the above terms in Eqs. (3) and (4) are known except for D , and thus an experimental value for D can be found from the measured T_1 values. Table II shows the values of D calculated by using the measured values of τ_c and T_1 for Mn^{2+} -doped CaF_2 sample No. 5. The determination of D is based on the following data: $N_p = 3.1 \times 10^{18}/\text{cm}^3$, $[S(S+1) \gamma_p^2 \hbar^2] (\text{Mn}^{2+}) = 3 \times 10^{-39} (\text{erg/G})^2$, $\omega_0 = 2\pi \times 10^7 \text{ rad/sec}$, $\gamma_n (F^{19}) = 2.52 \times 10^4/\text{G-sec}$.

Values for τ_c of the Eu^{3+} ions in the Eu^{3+} -doped CaF_2 sample were obtained in the same way. The $\tau_c^{1/4}$ dependence of T_1 was roughly satisfied in the temperature range 96 – 77°K . In Table III are listed the values of τ_c in this temperature range. The corresponding T_1 values were measured in the laboratory reference frame, with the polarizing \mathbf{B}_0 field parallel to the $[110]$ direction of the crystal. The calculation of D is based on the following data: N_p (Eu^{3+} -sample No. 1) = $2.86 \times 10^{19}/\text{cm}^3$, $[S(S+1) \gamma_p^2 \hbar^2] (\text{Eu}^{3+}) = 9.9 \times 10^{-40} (\text{erg/G})^2$. The agreement in the listed values for D in Tables II and III is reasonably good, considering that: there is a large uncertainty in N_p for each of these samples; that one sample is polycrystalline and was grown by us and

TABLE III. Calculations of the spin-diffusion constant D from data for τ_c and T_1 for Eu^{3+} -doped CaF_2 crystal.

$T^\circ\text{K}$	τ_c in 10^{-6} sec	T_1 (measured) in msec	D (calculated) in 10^{-12} cm^2/sec
96	2.2 ± 0.1	49 ± 1.5	1.22
88	3.5 ± 0.1	56 ± 1.5	1.20
77	6 ± 0.1	66 ± 1.5	1.15

the other is a single crystal and was grown commercially; and that there is no knowledge of how the paramagnetic centers are distributed in the crystals.

Theoretical calculations of the average diffusion constant D have been carried out by several different authors.^{1,16,17} From the most recent of these calculations,¹⁶ we have evaluated the average diffusion constant D for CaF_2 for the applied static magnetic field \mathbf{B}_0 along the [100], [110], and [111] crystal axes. These results are listed in Table IV.

From Table IV, a reasonable estimate of D for a polycrystalline CaF_2 sample is 5.1×10^{-12} cm^2/sec . Depending upon which of the two sets of experimental values of D is used for a basis of comparison (or possibly an average of the experimental values should be used), the measured value of the average diffusion constant D is smaller than the computed value by a factor of 3 to 4. This is quite a reasonable agreement considering the possible sources of error listed earlier in the experimental measurement of D , and the theoretical approximations that have been made. Among these approximations are: the replacement of C , which is angularly dependent by \bar{C} , its value averaged over a sphere; the replacement of the diffusion tensor $D^{\alpha\beta}$ by its average value D ; and the assumption that the paramagnetic centers are uniformly distributed throughout the CaF_2 crystal. Crude calculations show that even for a cubic lattice, the diffusion rate along the magnetic field \mathbf{B}_0 is about four times as rapid as perpendicular to it. There is also an experimental bias that tends to make the measured spin-lattice relaxation time T_1 longer than it really is. By plotting the quantity $\log\{[M_0 - M(t)]/M_0\}$ and fitting it with a best straight line, more weight is given to those regions in the crystal where the magnetization recovers more slowly, and there is a built-in bias towards finding a T_1 value that is larger than some mean

TABLE IV. Calculated values for the average diffusion constant D for CaF_2 for \mathbf{B}_0 along the [100], [110], and [111] crystal axes.

Direction of \mathbf{B}_0	D (10^{-12} cm^2/sec)
[100]	5.0
[110]	4.8
[111]	5.5

¹⁶ I. J. Lowe and S. Gade, Phys. Rev. **156**, 817 (1967).

¹⁷ G. R. Khutsishvili, Usp. Fiz. Nauk **87**, 211 (1965) [English transl.: Soviet Phys.—Usp. **8**, 743 (1966)].

average. This then tends to yield too small a value for D if N_p and \bar{C} are assumed known.

The experimentally determined $\tau_c^{1/4}$ dependence of T_1 also affords a test of Rorschach's¹⁸ theory of the diffusion-barrier radius b . In Rorschach's calculation, b is given by

$$b = [3 \langle \mu_p \rangle_z / \mu_n]^{1/4} a, \quad (6)$$

where $\langle \mu_p \rangle_z$ is the average magnetic moment of the paramagnetic ion that is effective in quenching diffusion, a is the lattice constant, μ_n is defined in terms of the nuclear local field B_l , $\mu_n \simeq B_l/a^3$. At "high" temperatures, $\langle \mu_p \rangle_z^2$ is given by

$$\langle \mu_p \rangle_z^2 = \frac{1}{3} \mu_p^2 [(2/\pi) \tan^{-1}(\tau_c/T_2)], \quad (7)$$

where T_2 is the nuclear spin-spin relaxation time, and μ_p represents the magnitude of the free-ion magnetic moment. The magnitude of b can be calculated from Eqs. (6) and (7) if τ_c is known. Experimentally, the available values of τ_c and its dependence on T_1 indicate that T_1 belongs to the diffusion-limited case. This in turn requires that the parameter δ ($\delta = \beta^2/2b^2$, see LT for discussion) be at least equal to or larger than unity.

TABLE V. The ratio of T_1^r/T_1 for the Ce^{3+} -doped CaF_2 sample No. 2 in the short τ_c region.

Temperature ($^\circ\text{K}$)	300	245	227	195	90	77	60	50
T_1^r/T_1	0.85	1.17	1.16	1.27	1.27	1.27	1.32	1.30

This requirement places an upper limit on the experimental value of b , namely, $b < \beta/\sqrt{2}$. But calculations show that in both the Eu^{3+} - and Mn^{2+} -doped samples, the magnitudes of b given by Rorschach's formula are larger than the experimentally determined upper limits by at least a factor of 2. This discrepancy seems to indicate that diffusion is not effectively quenched except in those regions that are closer to the paramagnetic center than have previously been estimated.

In the measurement of T_1 as a function of temperature, for the Eu^{3+} - and Mn^{2+} -doped samples, T_1 was found to increase monotonically as temperature was lowered from room temperature ($\sim 300^\circ\text{K}$), indicating that $\omega_0\tau_c > 1$ throughout the temperature range. But in the case of the Ce^{3+} -doped samples, the situation is quite different. In the temperature range 300–50°K, T_1 was found to decrease monotonically for decreasing temperature, and from 4.2 to 2°K, T_1 was found to increase for decreasing temperature. We could not measure T_1 in the range of 50 to 4.2°K because our cryostat did not cover this temperature range. Log T_1 for the Ce^{3+} -doped CaF_2 sample No. 2 is plotted against log T in Fig. 4. The general behavior indicates that a T_1 minimum must occur somewhere within the temperature range of 50 to 4.2°K. By extrapolating the two

¹⁸ A. G. Rorschach, Jr., Physica **30**, 38 (1964).

plotted curves and finding where they cross, we conclude that the T_1 minima should occur at about $T=15^\circ\text{K}$, and that the value of τ_c at that temperature should be of the order of 10^{-8} sec. Therefore, well above 15°K , where τ_c is much shorter than 10^{-8} sec, the condition that $1 \gg \omega_0 \tau_c \gg \omega_1 \tau_c$ should be valid. For this condition, it is shown in Sec. III B of LT that the ratio T_1^r/T_1 should vary continuously from 0.86 (rapid-diffusion case) to 1.62 (diffusion-limited case) as the temperature decreases. For the Ce^{3+} -doped CaF_2 sample No. 2, the experimentally measured ratio of T_1^r/T_1 is listed in Table V for eight different temperatures. These results support the theory in a qualitative manner, and demonstrate that under certain conditions $T_1^r > T_1$. At higher temperatures, T_1^r and T_1 are nearer to the field-independent rapid diffusion

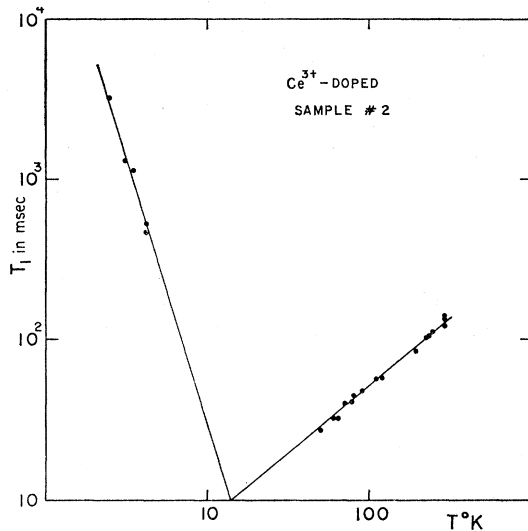


FIG. 4. $\log T_1$ versus $\log T$ for Ce^{3+} -doped CaF_2 sample No. 2.

region. As the temperature is lowered, T_1 and T_1^r are shifted into the diffusion-limited region, which is still field-independent. In order for T_1^r/T_1 to be about 1 in the rapid diffusion region, the spin-diffusion barrier in the rotating reference frame b^r must be about equal to the spin-diffusion barrier in the laboratory reference frame b . [See Eqs. (34) and (73) of LT.] In order for $T_1^r/T_1 > 1$ in the diffusion-limited region, the spin-diffusion constant in the rotating reference frame D^r must be smaller than the spin-diffusion constant in the laboratory reference frame D .

B. N_p Dependence of the Nuclear Spin-Lattice Relaxation Time

In the formulas of LT for $(T_1)^{-1}$ and $(T_1^r)^{-1}$ for the diffusion-limited and rapid-diffusion cases, the dominant terms are proportional to N_p , the number of paramagnetic centers per unit volume. However, as β [defined in Eq. (5)] approaches the value of R , LT

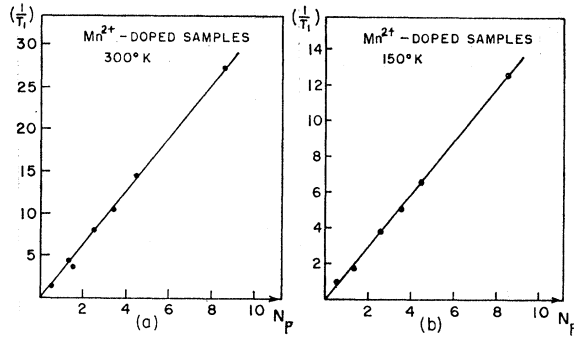


FIG. 5. T_1^{-1} versus N_p for Mn^{2+} -doped CaF_2 samples. N_p is in arbitrary units. (a) $T=300^\circ\text{K}$, (b) $T=150^\circ\text{K}$.

predicts that the dominant terms in the formulas for for $(T_1)^{-1}$ and $(T_1^r)^{-1}$ should be proportional to $(N_p)^{4/3}$. To test these predictions, the dependence of $(T_1)^{-1}$ and $(T_1^r)^{-1}$ upon N_p was studied.

In Figs. 5(a) and 5(b), the measured values of $(T_1)^{-1}$ at 300 and 150°K are plotted against N_p for the Mn^{2+} -doped CaF_2 samples. Both sets of points are well fitted by straight lines and verify the dependence of $(T_1)^{-1}$ upon N_p . This result is consistent with the conclusions of Sec. III A, where it was found that T_1 at 150°K must belong to the diffusion-limited case because of its $\tau_c^{1/4}$ dependence.

In Fig. 6, the measured values of $\log T_1^r$ at 154°K are plotted against $\log N_p$ for four representative samples of Mn^{2+} -doped CaF_2 crystals. The measurements were made at 154°K using a rotating magnetic field B_1 equal to 16 G. The four points are well fitted by a line of slope -1.35 . From this, we conclude that T_1^r is proportional to $(N_p)^{-1.35 \pm 0.1}$ and that the diffusion-vanishing case applies to the nuclear relaxation process in the rotating reference frame at 154°K . As a check to see whether the nuclear relaxation process in the rotating reference frame does belong to the diffusion-vanishing case, the criteria of LT ought to be verified,

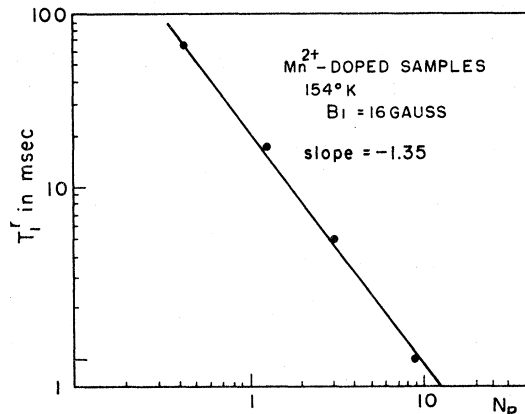


FIG. 6. $\log(T_1^r)$ versus $\log(N_p)$ for Mn^{2+} -doped CaF_2 samples, Nos. 1, 5, 7, and 8. Measurements were made at 154°K with a rotating magnetic field $B_1=16$ G.

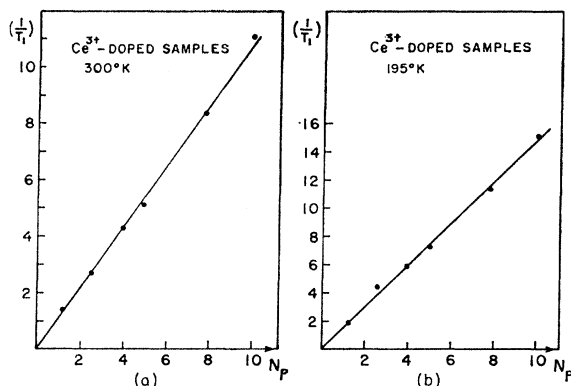


FIG. 7. $(T_1)^{-1}$ versus N_p for Ce^{3+} -doped CaF_2 crystals. (a) $T=300^\circ\text{K}$, (b) $T=195^\circ\text{K}$.

that,

$$\Delta^r = [(\beta^r)^2/2R^2] > 1, \quad (8)$$

where

$$\beta^r = (\bar{C}^r/D^r)^{1/4}, \quad (9)$$

$$\bar{C}^r = \gamma_p^2 \gamma_n^2 \hbar^2 S(S+1) \left[\frac{4}{15} \left(\frac{\tau_c}{1+\omega_1^2 \tau_c^2} \right) + \frac{1}{5} \left(\frac{\tau_c}{1+\omega_0^2 \tau_c^2} \right) \right], \quad (10)$$

$$D^r = D/2, \quad (11)$$

$$\omega_1 = \gamma_n B_1. \quad (12)$$

Figure 3 yields a value for τ_c of 2.5×10^{-6} sec for Mn^{2+} ions in CaF_2 at 154°K . Thus, for Mn^{2+} ions in CaF_2 , β^r has a value of about 100 Å. Therefore, the condition that $\Delta^r > 1$ is satisfied for all the Mn^{2+} -doped CaF_2 samples (see Table I) whose data were used in Fig. 6.

The case of the Ce^{3+} -doped CaF_2 crystals is very different. In Figs. 7(a) and 7(b), values of T_1^{-1} measured at 300 and 195°K are plotted against N_p of the Ce^{3+} -doped CaF_2 crystals. In Fig. 8, $\log T_1^r$ measured at 195°K with a locking field B_1 of 24 G is plotted against $\log N_p$ of the Ce^{3+} -doped CaF_2 crystals. All three curves show $(T_1)^{-1}$ and $(T_1^r)^{-1}$ to be proportional to N_p at the measuring temperatures. This result is consistent with those of Sec. IIIA for the following reason. There, it was determined that at $T > 50^\circ\text{K}$, τ_c of the Ce^{3+} ions in CaF_2 is short in comparison to $(\omega_0)^{-1}$. In the short τ_c region, both β and β^r are small in comparison to R so that Δ and Δ^r are much less than 1. Therefore, both T_1 and T_1^r should be either in the diffusion-limited or rapid-diffusion regions. In both these regions, the dominant terms in the formulas for $(T_1)^{-1}$ and $(T_1^r)^{-1}$ are proportional to N_p . In fact, it was found in the measurement of the ratio T_1^r/T_1 that our results corresponded to T_1^r and T_1 being in the transition region between the two limiting cases.

In concluding this section, it should be pointed out that when choosing data for the Mn^{2+} -doped CaF_2 samples to test the concentration dependence of T_1^r in the diffusion-vanishing case, we limited data to meas-

urements carried out in the temperature range of 77 to 178°K . The reasons for this limitation are the following:

(1) At higher temperatures, the values of τ_c for Mn^{2+} -ions are short compared to ω_1^{-1} for the largest attainable B_1 fields in our laboratory, and the corresponding values for β and β^r are too small to satisfy the condition for the diffusion-vanishing case.

(2) At lower temperatures (77°K and below), an additional concentration dependence of T_1 appears due to the dependence of τ_c upon N_p in the more strongly doped samples. As suggested in Sec. IIIA, at low temperatures, the spin-spin dipolar interaction among the paramagnetic ions (proportional to the inverse third power of the average impurity separation) may dominate the spin-lattice interaction contribution to the correlation time τ_c , in the low-frequency region. Thus, τ_c may acquire an impurity concentration dependence which could be confused with the unique $N_p^{-4/3}$ dependence of T_1 for the diffusion-vanishing case.

If the correlation time τ_c were completely determined by the spin-spin dipolar interaction, the over-all concentration dependence of T_1 would in principle be varying continuously from $N_p^{-11/6}$ to $N_p^{-5/4}$ and back to N_p^{-2} as T_1 shifts from the diffusion-vanishing case to the diffusion-limited case and on to the rapid-diffusion case. In practice this wide range of N_p dependence involves such strenuous experimental conditions that it is hopelessly impossible to verify in a continuous fashion. Our measurements of T_1 for Mn^{2+} -doped samples at He temperature indicate that T_1 is proportional to $N_p^{-1.6}$, giving some support to the evidence of possible additional concentration dependence at lower temperature due to strong spin-spin interaction among the paramagnetic centers.¹⁹

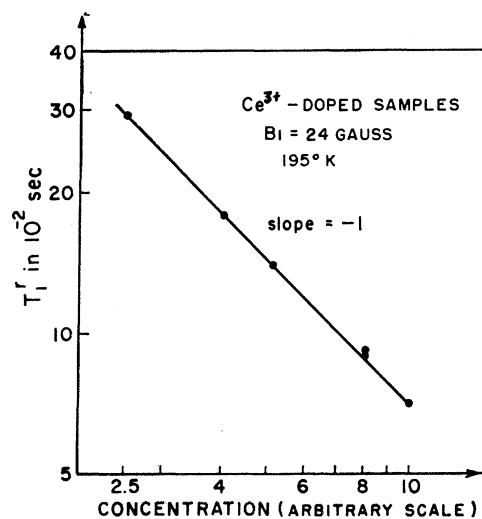


FIG. 8. $\log(T_1^r)$ versus $\log(N_p)$ for Ce^{3+} -doped CaF_2 crystals. Measurements were made at 195°K with a rotating magnetic field $B_1=24$ G.

¹⁹ O. S. Leifson and G. D. Jeffries, Phys. Rev. **122**, 1781 (1961).

TABLE VI. Magnetic field dependence of T_1 for $\omega_0\tau_c \gg 1$. The table may also be applied to T_1^r , when $\omega_1\tau_c \gg 1$, by replacing δ by δ^r , Δ by Δ^r , and B_0 by B_1 .

Case	Condition	Exponential dependence on B_0
Diffusion vanishing	$\delta \gg 1, \Delta \geq 1$	1
Diffusion limited	$\delta \gg 1, \Delta \ll 1$	$\frac{1}{2}$
Rapid diffusion	$\delta \ll 1, \Delta \ll 1$	2

C. Field Dependence of the Nuclear Spin-Lattice Relaxation Time

The investigation of the magnetic field dependence of nuclear spin-lattice relaxation times of crystals doped with paramagnetic centers is always complicated by the uncertainty of the field dependence of τ_c . However, by carrying out relaxation-rate experiments in the rotating reference frame, this complication is eliminated.

The magnetic field dependence of T_1^r is contained only in \bar{C}^r , listed in Eq. (10). In the short τ_c region, the $\omega_1\tau_c$ term in the denominator of \bar{C}^r can be dropped in comparison to unity, and T_1^r is field-independent regardless of what case it may be in. This field independence of T_1^r was verified by measurements of T_1^r for the Ce^{3+} -doped CaF_2 samples at temperatures above 50°K , where it is known that $\omega_0\tau_c \ll 1$. The measured values of T_1^r for different Ce^{3+} -doped CaF_2 samples remained constant as the locking field B_1 in the rotating frame was varied from 25 to 7.5 G.

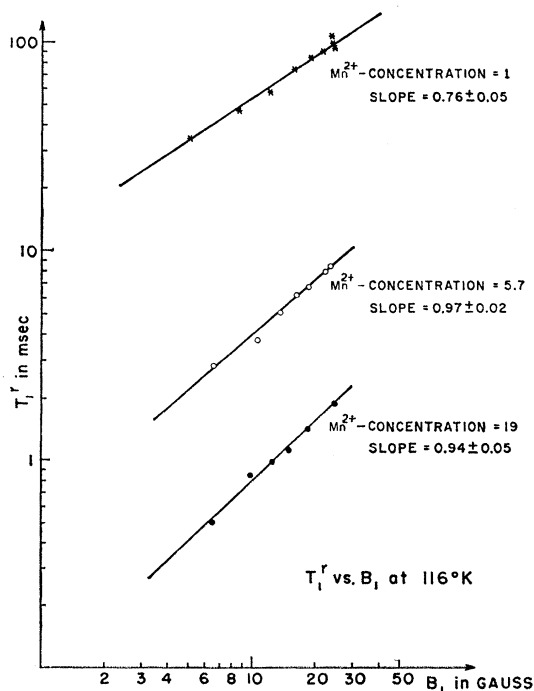


FIG. 9. $\text{Log}(T_1^r)$ versus $\text{log}B_1$ for three different Mn^{2+} -doped CaF_2 crystals. $T = 116^\circ\text{K}$.

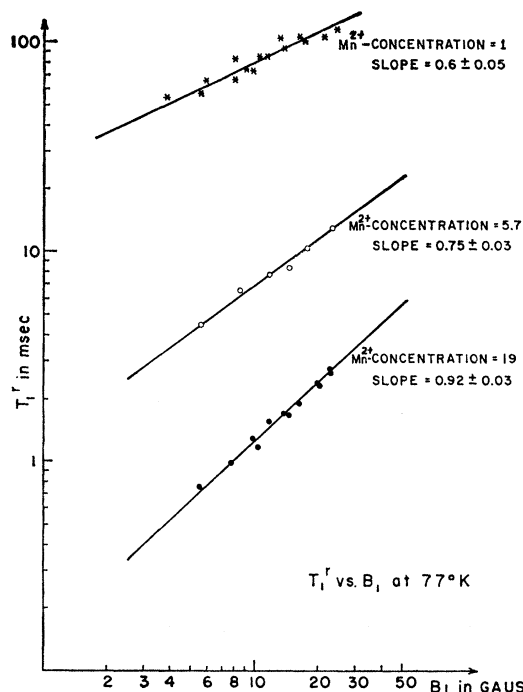


FIG. 10. $\text{Log}(T_1^r)$ versus $\text{log}B_1$ for three different Mn^{2+} -doped CaF_2 crystals. $T = 77^\circ\text{K}$.

For the long τ_c region, the field dependence of the dominant terms in the formulas of LT for T_1 and T_1^r are given in Table VI. To test Table VI, values of T_1^r for several crystals were measured for many values of the locking field B_1 . The measurements were made at fixed temperatures, where it was known that τ_c satisfied the condition $\omega_1\tau_c > 1$. The field dependence of T_1^r was determined from the slope of the $\text{log} T_1^r$ versus $\text{log} B_1$ curves.

The $\text{log} T_1^r$ versus $\text{log} B_1$ for three Mn^{2+} -doped CaF_2 crystals is plotted in Fig. 9. The relative values for N_p for the three crystals are 1, 5.7 and 19, and the measurements were made at a temperature of 116°K , where τ_c is estimated to have a value of 7×10^{-6} sec (see Fig. 3). All three curves in Fig. 9 appear to be reasonably linear, the scatter of points being due to inaccuracies in measuring T_1^r and B_1 . These inaccuracies are estimated to total about 10%. The $\text{log} T_1^r$ versus $\text{log} B_1$ curves are expected to be linear only when T_1^r is well within either of its three limiting cases. In the transition regions one expects to see some curvature to the

TABLE VII. Magnetic field dependence of T_1^r for three Mn^{2+} -doped CaF_2 crystals. Measurements were made at 116°K .

Sample number	N_p (relative)	Δ^r	Exponential dependence on B_1
8	1	0.4	0.76 ± 0.05
5	5.7	1.2	0.97 ± 0.05
1	19	2.8	0.94 ± 0.05

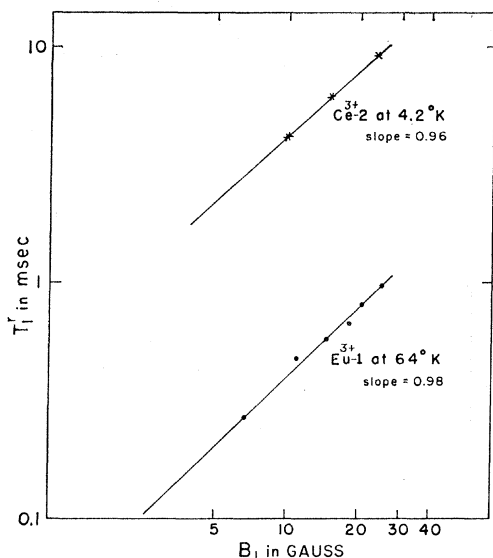


FIG. 11. $\log(T_1^r)$ versus $\log B_1$ for the Ce^{3+} -doped CaF_2 crystal No. 2 at 4.2°K , and the Eu^{3+} -doped CaF_2 crystal at 64°K .

$\log T_1^r$ versus $\log B_1$ curves; however, this should be negligible over a small enough range of examination. This appears to be the case for our data. The magnetic field dependence measured from the curves of Fig. 9 is summarized in Table VII. Also listed are the estimated values of Δ^r for the three samples for a rotating magnetic field value B_1 of 16 G. For these estimations, we have set $\tau_c = 7 \times 10^{-6}$ sec and $D^r = 2 \times 10^{-12}$ cm^2/sec . The values of $\Delta^r > 1$ for samples No. 1 and 5 of Table VII place T_1^r for them in the diffusion-vanishing case. The listed exponential dependence on B_1 of 0.94 and 0.97 is in good agreement with the predicted value of 1.0 and seems to verify that part of the theory. The value of $\Delta^r = 0.4$ for sample 8 places it midway between the diffusion-vanishing case and the diffusion-limited case, and its listed exponential dependence on B_1 of 0.76, which is midway between 1 and 0.5, agrees with this conclusion.

Measurements of T_1^r for these same three crystals were also made at 77°K , and the results are plotted in Fig. 10. For these samples, τ_c at 77°K is longer than it is at 116°K so that Δ^r at 77°K for these samples is

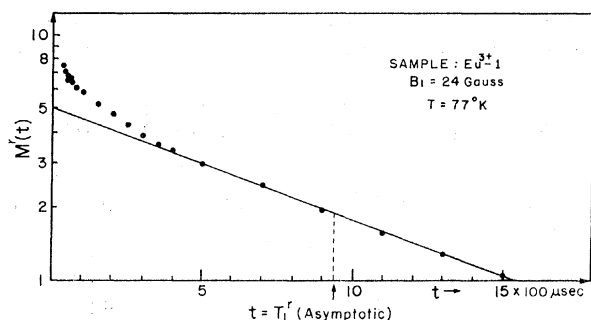


FIG. 12. $\log M^r(t)$ versus t for a Eu^{3+} -doped CaF_2 crystal at 77°K , $B_1 = 24$ G.

smaller than at 116°K . We thus should expect samples 1 and 5 to be somewhere between the diffusion-vanishing region and the diffusion-limited region, with the exponential dependence of T_1^r upon B_1 being smaller since its value of Δ^r is smaller. This is indeed seen to be the case, as shown in Table VIII. Sample 8, which was in between the diffusion-vanishing region and the diffusion-limited region when at 116°K should be closer to or in the diffusion-limited region at 77°K , and its exponential dependence of T_1^r upon B_1 should be somewhere between 0.76 and 0.5. This is also the case, as is shown in Table VIII. The analysis of the data at 77°K is consistent with that at 116°K . The somewhat larger scatter in the T_1^r data for sample 8 at 77°K arises from the difficulty in producing large, fixed amplitude, rotating magnetic fields with long time durations.

A similar set of measurements has been carried out on the Eu^{3+} -doped CaF_2 sample at a temperature of 64°K , and the Ce^{3+} -doped CaF_2 No. 2 at 4.2°K . The results of these measurements are plotted in Fig. 11, in the form of $\log T_1^r$ versus $\log B_1$. Both sets of data are well fitted by straight lines with slopes near 1, indi-

TABLE VIII. Magnetic field dependence of T_1^r for three Mn^{2+} -doped CaF_2 crystals. Measurements were made at 77°K .

Sample number	N_p (relative)	Exponential dependence on B_1
8	1	0.6 ± 0.05
5	5.7	0.75 ± 0.03
1	19	0.92 ± 0.03

cating that they are both in the diffusion-vanishing region.

D. Initial Nonexponential Decay of Magnetization along the Rotating Magnetic Field

It was found during the T_1^r measurements on all CaF_2 samples doped with paramagnetic centers that for $\omega_1 \tau_c > 1$, the nuclear magnetization along the rotating magnetic field exhibited a nonexponential decay in its initial magnetization. It was found that the magnetization along the rotating magnetic field decayed at a rate proportional to $t^{1/2}$, and that this behavior was exhibited for a period as long as one-third of the asymptotic T_1^r value. (t is the time measured from the end of the initiating radio-frequency pulse that nutates the magnetization from along B_0 to perpendicular to it.) It was found that as the temperature was lowered from those values where the $t^{1/2}$ rate of decay was most pronounced, that the $t^{1/2}$ law became less and less pronounced, even though τ_c continued to increase.

An example of the initial nonexponential decay of magnetization is shown in Fig. 12, where $\log M^r(t)$ is plotted against t for the Eu^{3+} -doped CaF_2 crystal at 77°K . In Fig. 13, the quantity $[M^r(0) - M^r(t)]/M^r(0)$ is plotted versus $t^{1/2}$ for the same sample for tem-

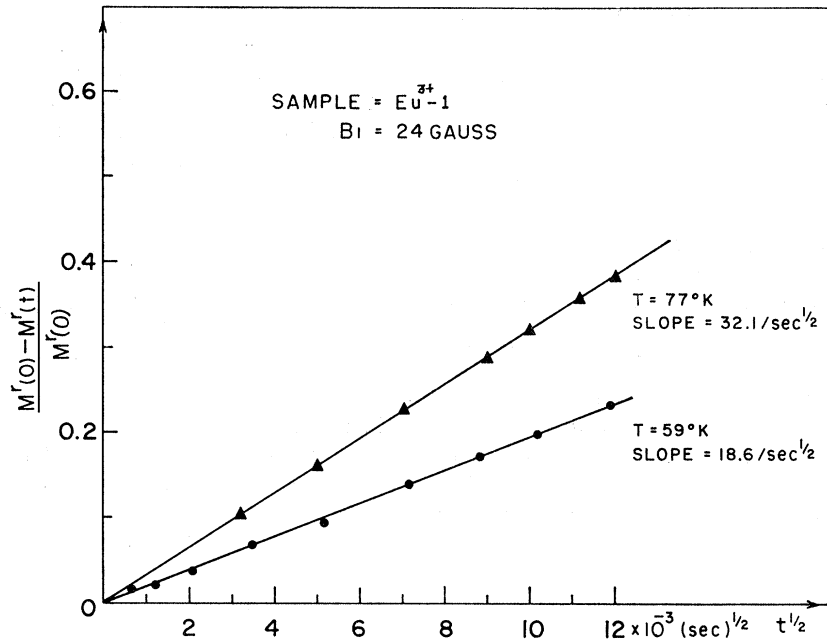


FIG. 13. $[M^r(0) - M^r(t)]/M^r(0)$ versus $t^{1/2}$ for the Eu^{3+} -doped CaF_2 crystal for $B_1 = 24$ G. Upper curve corresponds to $T = 77^\circ\text{K}$. Lower curve corresponds to $T = 59^\circ\text{K}$.

peratures of 77 and 59°K, and a locking field of 24 G. The initial value of the magnetization $M^r(0)$ was found by extrapolating the $M^r(t)$ versus $t^{1/2}$ curve back to $t=0$ for both the 77 and 59°K curves. Both sets of data in Fig. 13 are well fitted by straight lines; the line for the data at 77°K has a slope of 32.1/sec^{1/2} and the line for the data at 59°K has a slope of 18.6/sec^{1/2}.

Blumberg²⁰ has pointed out that for T_1 measurements in crystals containing paramagnetic centers, the diffusion-limited case can be distinguished from the rapid diffusion case by the initial rate of change of the magnetization following saturation. He argued that in the process of the measurement of T_1 , for a short time after the nuclear spin is saturated (for instance, by a 90° pulse), the magnetization gradient across the sample is zero and the only rate of change of magnetization is due to direct relaxation. He concluded that if the direct relaxation rate is fast enough outside the spin-diffusion barrier (the condition for the diffusion-limited case), an appreciable amount of nuclear magnetization can grow by the direct relaxation process, and that the initial growth of the nuclear magnetization is proportional to $t^{1/2}$.

The ideas described in the above paragraph may also be used to explain the $t^{1/2}$ behavior of $M^r(t)$ for short times. The difference between the case of relaxation in the laboratory reference frame and the rotating reference frame is that for the rotating reference frame case, the initial magnetization throughout the sample is constant, and the magnetization gradient is set up as direct relaxation causes the magnetization to decay to a value close to zero. In particular, when T_1^r is given by the diffusion-vanishing case, the direct relaxation rate is at its largest value relative to the diffusion rate, and a

large portion of the decay curve for $M^r(t)$ should obey the $t^{1/2}$ law, which is what we have found. As the temperature is lowered and the direct relaxation rate decreases, the portion of the decay of $M^r(t)$ that obeys the $t^{1/2}$ law should become smaller, which also agrees with our experimental results. In the extreme short-correlation-time region ($\omega_1\tau_c < \omega_0\tau_c < 1$), no deviation from a simple exponential decay of the nuclear magnetization was observed, either in the laboratory reference frame or the rotating reference frame. This was probably due to the fact that the $t^{1/2}$ region of the decay of the magnetization is too short to be observed.

Blumberg's formula for the initial recovery of the magnetization following saturation is given by²⁰

$$M_z(t) = \frac{4}{3}\pi^{3/2}M_0N_p(\bar{C}^r)^{1/2}t^{1/2}. \quad (13)$$

In deriving the above equation, Blumberg assumed that the direct relaxation process was spherically symmetric. We have carried out a derivation of the initial behavior of $M_z(t)$, using the proper angular dependence for the direct relaxation process and have gotten the same equation as listed above, along with a small correction factor. Applying the same technique to the initial behavior of $M^r(t)$, we find that

$$M^r(t) = M^r(0) \left[1 - \frac{4}{3}\pi^{3/2}N_p(\bar{C}^r)^{1/2}t^{1/2} \right], \quad (14)$$

where $M^r(0)$ is the initial value of the magnetization.

From Eq. (14), the slope of the curve of $[M^r(0) - M^r(t)]/M^r(0)$ is given by

$$S^r = \frac{4}{3}\pi^{3/2}N_p(\bar{C}^r)^{1/2}. \quad (15)$$

If S^r can be experimentally measured, and \bar{C}^r computed from other information, an effective value for N_p can be computed from Eq. (15). All this information is available for the Eu^{3+} -doped sample at 77°K. The

²⁰ W. E. Blumberg, Phys. Rev. **119**, 79 (1960).

upper curve of Fig. 13 yields $S^r = 32.1/\text{sec}^{1/2}$. Table III yields a value of $\tau_c = 6 \times 10^{-6}$ sec, from which the computed value of \bar{C}^r is 7.12×10^{-38} cm⁶/sec for $B_1 = 24$ G. The computed value of N_p is $1.6 \times 10^{19}/\text{cm}^3$, as compared to the value of $2.85 \times 10^{19}/\text{cm}^3$ supplied by the manufacturer of the crystal.¹¹ If this effective value of N_p were used to calculate D in Sec. IIIA, instead of the value supplied by the manufacturer of the crystal, the computed value of D would have been larger by a factor of 2.18 than those given in Table III, and in closer agreement with the value calculated in Ref. 16.

IV. CONCLUSIONS

The results of these experiments give quantitative support to current theories of nuclear spin relaxation via paramagnetic centers where spin diffusion plays a part. In particular, the measured value for the spin-diffusion constant in CaF₂ agrees reasonably well with its current theoretical value. The spin-diffusion vanish-

ing case, predicted in LT, has been found, and the dependence of T_1 upon the magnetic field, τ_c and N_p , has been verified for both this case and the diffusion-limited case. In these experiments, the technique of studying relaxation in the rotating reference frame has been extremely useful, for it has allowed us to find T_1 and thus estimate τ_c . It has also allowed us to work in regions where the direct spin-lattice relaxation rate is very rapid without having an extremely high concentration of paramagnetic centers. This in turn has allowed us to verify Blumberg's prediction of how the nuclear spin system should relax when there is zero magnetization gradient in the sample.

ACKNOWLEDGMENT

One of us (I.J.L.) wishes to acknowledge the hospitality of the Physics Division of the Aspen Institute for Humanistic Studies, where part of this paper was written.

Random-Walk Models of Photoemission*

STEVEN W. DUCKETT

Aerospace Corporation, El Segundo, California

(Received 11 September 1967)

An exact solution in closed form is given for the photoyield in the isotropic random-walk model of photoemission. The proof makes use of a theorem of importance in the theory of queues and ladder-point variables. The effect of reflection of the photoelectrons at the interface is also treated. A recursion relation for the probability of emission on the n th step P_n is derived from the expression for the photoyield. Numerical values of the photoyield and the P_n 's are tabulated for numerous values of the relevant parameters, and these numbers are compared with the results of approximate expressions. The exact photoyield values are in good correspondence to a slightly modified version of a formula derived by Kane. A simple approximation is also given for the values of the P_n 's.

I. INTRODUCTION

PHOTOELECTRIC emission is a two-step process, involving the creation of a free electron in the interior of the solid and the eventual escape of this electron through the surface into the vacuum. The transport part of the problem has been treated as a random-walk phenomenon and both Monte Carlo results^{1,2} and approximate analytical formulas³⁻⁶ have been given for the photoemission. However, as this paper shows, an exact closed-form expression can be obtained for the photoyield in the random-walk model.

In addition, a formula for the probability of escape after exactly n collisions P_n is expressed in a form suitable for machine calculation, and the first twelve P_n 's have been calculated for numerous values of the absorption and scattering parameters. These probabilities are compared to the results of the approximate calculations, and it is shown that some rather simple formulas give very good approximations to the exact results.

II. RANDOM-WALK MODEL

The model considers an electron, created at (x, y, z) in the solid, that undergoes an isotropic random walk. The problem is to compute the probability that the electron will pass through the plane $x=0$ before its energy has been reduced to the point where it is impossible for the electron to escape. This energy loss usually occurs suddenly due to pair creation, electron-hole recombination, or the ionization of an impurity in the lattice. We will call the energy-loss event "absorption"

* This work was supported by the U.S. Air Force under Contract No. AF 04(695)-1001. Some of the calculations were begun when the author was a Ph.D. candidate at Cornell University.

¹ R. Stuart, F. Wooten, and W. E. Spicer, Phys. Rev. **135**, A495 (1964).

² R. Stuart and F. Wooten, Phys. Rev. **156**, 364 (1967).

³ S. Duckett and P. Metzger, Phys. Rev. **137**, A953 (1965).

⁴ E. O. Kane, Phys. Rev. **147**, 335 (1966).

⁵ P. Beckman, Phys. Rev. **150**, 215 (1966).

⁶ P. J. Roberts, Phys. Rev. Letters **18**, 823 (1967).